

PFC/JA-85-38

**TURBULENT STABILIZATION OF THE
TEARING MODE IN TOKAMAK PLASMAS**

Esarey, E.; Freidberg, J.P.; Molvig, K.;

Beasley*, C.O., Jr.; Van Rij*, W.I.

November, 1985

Plasma Fusion Center
Massachusetts Institute of Technology
Cambridge, Massachusetts 02139 USA

* present address: Oak Ridge National Laboratory, Oakridge, TN 37830

Submitted for publication in: Physics of Fluids

TURBULENT STABILIZATION OF THE TEARING MODE IN TOKAMAK PLASMAS

E. ESAREY, J.P. FREIDBERG and K. MOLVIG

Plasma Fusion Center and Department of Nuclear Engineering

Massachusetts Institute of Technology

Cambridge, Massachusetts 02139

and

C.O. BEASLEY, JR. and W.I. VAN RIJ

Oak Ridge National Laboratory

Oak Ridge, Tennessee 37830

ABSTRACT

The effect of turbulent electron diffusion from stochastic electron orbits on the stability of low-beta fluctuations is considered through the use of the Normal Stochastic Approximation. A set of coupled, self-adjoint equations is derived for the fluctuation potentials $\tilde{\phi}$ and $\tilde{A}_{||}$. Solutions to this set of equations describe both unstable finite- β drift waves when analyzed for high m modes and the tearing mode when analyzed for low m modes. For the tearing mode, it is shown that stability is obtained for sufficiently large values of the diffusion coefficient. Provided $D_e \sim 1/n$, this implies that a density threshold must be surpassed before the tearing mode is observed. Physically, turbulent electron diffusion prohibits the formation of a perturbed current within a finite region about the rational surface. At higher densities, the inclusion of a finite electrostatic potential, $\tilde{\phi}$, gives an additional stabilizing term to the dispersion relation, which physically represents ion inertial effects. This ion inertial effect implies that, in the absence of diffusion, the tearing mode is stabilized for ion betas, β_i , above some critical value.

I. Introduction

Tearing modes are a subject of current interest in plasma physics due to their role in both space and laboratory plasma behavior. In space plasmas, tearing modes are an important destabilization mechanism in spontaneous magnetic reconnection phenomena, such as in the onset of substorms in the Earth's magnetotail^{1,2}. In laboratory plasmas, such as in a tokamak, tearing modes play an important role in the onset of major plasma disruptions. It is generally agreed that major disruptions must be totally suppressed in an actual fusion reactor in order to prevent excessive damage to the first wall. Currently, the most widely accepted theoretical model of major disruptions features low poloidal number (low m) tearing modes, which saturate to produce magnetic islands. It is possible for such magnetic islands to overlap and thus form large stochastic magnetic regions, which enhance particle diffusion, and, in the case of major disruptions, lead to catastrophic plasma confinement loss³⁻⁶. Hence, control of such disruptions requires the elimination or, at least suppression, of these tearing mode islands.

Recent experimental results on Alcator-C indicate the existence of a density threshold which must be surpassed before the $m = 2$ tearing mode is observed⁷. Such an observation is inconsistent with the previous resistive magnetohydrodynamic (MHD) theories of the tearing mode. Traditionally, the tearing mode has been analyzed using resistive MHD theory, which predicts instability for $\Delta' > 0$, independent of plasma density³. Here Δ' is the jump in the logarithmic radial derivative of the perturbed magnetic potential, $\tilde{A}_{||}$, across the rational surface. This is determined by integrating the ideal MHD equation for the vector potential from the external region inward towards the rational surface. Typically, experimental profiles indicate $\Delta' > 0$, and hence the $m = 2$ tearing mode should be observed according to resistive MHD. The existence of a density threshold before the onset of instability, which is in qualitative disagreement with resistive MHD, has motivated the present work.

In this paper, a fully kinetic approach to the tearing mode is used, which includes the effects of turbulent electron diffusion and treats the tearing mode as an electromagnetic fluctuation. The end effect of the turbulent electron diffusion is to stabilize the tearing

mode at sufficiently large values of the diffusion coefficient⁸. This would imply the existence of a density threshold if the local electron diffusion coefficient scales inversely with density, $D_e \sim 1/n$. Physically, electron diffusion prohibits the tearing region from becoming too small, whereas in resistive MHD the layer thickness becomes as thin as necessary and only limits the growth rate without affecting stability. Electron diffusion prohibits the formation of a perturbed parallel current channel narrower than the correlation distance, $x_c = (D_e/k'_{\parallel}v_e)^{1/3}$. This flattening of the perturbed current thus cuts into the available free energy driving the tearing mode (represented by Δ'), hence reducing the available energy to $\Delta'(x_c)$ (as opposed to $\Delta'(0)$ in resistive MHD). Here, $\Delta'(x_c)$ is the difference between the logarithmic derivative of \tilde{A}_{\parallel} evaluated at a distance x_c from the rational surface and that value at a distance of $-x_c$. For typical experimental profiles, $\Delta'(x)$ is a decreasing function of the distance from the rational surface, x . Hence, stability occurs when $x_c > W$, W being the distance where $\Delta'(W) = 0$.

The effects of a finite electrostatic potential, $\tilde{\phi}$, on the tearing mode are investigated and found to be stabilizing. (The previous paper on this subject by the authors treated the tearing mode as a primarily magnetic fluctuation⁸.) Physically, the relevant stabilizing terms involving the electrostatic potential represent ion inertia. This mechanism is completely independent of electron diffusion. In fact, when the diffusion is neglected, the tearing mode is stabilized when $\beta_i(\tau L_s/L_n)^{1/2} > \Delta'(0)$, indicating stability at sufficiently high plasma beta. Here, τ is the temperature ratio, L_s is the shear length, L_n the density scale length, and β_i is the ratio of ion pressure to magnetic pressure. A result identical to this was obtained previously by Basu and Coppi⁹.

Physically, this stabilizing effect represents that portion of the available magnetic energy driving the tearing mode which must be used to maintain the ion motion. In the kinetic theory description, the tearing mode is an unstable oscillation with a real frequency ($\omega = \omega_{*e}$). Finite ion inertia requires energy to maintain the ion oscillation and, hence, becomes a stabilizing effect. In contrast, for the purely growing modes of the resistive MHD description, no ionic energy is required by the perturbation itself, and ion inertia does not influence stability, but only the magnitude of the growth rate. In the kinetic picture, the tearing mode is actually interpreted as an electron drift wave under modification of

the equilibrium current gradient. This current gradient introduces an additional energy source which drives the low m “Drift-Tearing” modes unstable. By treating this mode as an electromagnetic fluctuation, it is found that the inclusion of a finite electrostatic potential indicates that the tearing mode can be stabilized at sufficiently high densities, in addition to the stability at low densities.

Section II discusses the mathematical model used in this treatment of the tearing mode and gives the derivation of a coupled, self-adjoint system of equations for the fluctuation potentials \tilde{A}_{\parallel} and $\tilde{\phi}$. This includes a brief discussion of the Normal Stochastic Approximation (NSA), which enables the effects of turbulent electron diffusion to be treated in a self-consistent manner¹⁰. Section III.A describes which approximations are necessary to obtain the resistive MHD results for the tearing mode from the above set of coupled equations. The remainder of Section III returns to the problem of the kinetic tearing mode and aims at solving the full set of kinetic equations for $\tilde{\phi}$ and \tilde{A}_{\parallel} . Included is a formal analytic proof that the tearing mode is stabilized for sufficiently large values of the diffusion coefficient, D_e , for a system which is resistive MHD unstable, $\Delta'(0) > 0$. A variational calculation of the dispersion relation for the electromagnetic tearing mode is also presented. Numerical results to the full kinetic description are presented in Section IV, which show good agreement to the analytical calculations of the previous section.

II. Mathematical Model

In a tokamak plasma, the effects of plasma turbulence play a major role in determining the overall properties of plasma transport. Thus, it is clear that any correct theory of plasma transport must include turbulence. Likewise, in the study of plasma instabilities, it is apparent that the effects of plasma turbulence on the instability itself may play an important role. In particular, in this study the major turbulent effect to be considered is that of electron spatial diffusion.

A mathematical model is developed, based on the Normal Stochastic Approximation (NSA), which includes self-consistently the effects of turbulent electron diffusion¹⁰. In particular, the electron response is given by applying the NSA to the drift kinetic equation. The basic assumption utilized here is that the electrons experience normally distributed stochastic orbits resulting from the overlap of phase space islands, which thus lead to the exponentiation of neighboring particle trajectories. These stochastic electron orbits are the direct result of the presence of drift wave microturbulence. The NSA makes use of the observation that for electrons exhibiting stochastic orbits, the exact orbit perturbations exhibit pathologically complex, fine-scale structures, which are produced directly from relatively simple, long-scale wave perturbations. Since the spatial structure characterizing the electron orbits is much finer than that characterizing the wave potentials, it is possible to separate the statistics of the particle orbits from the statistics of the wave potentials by a coarse-graining procedure. The end result is that the nonlinear effects of turbulence are represented by the appearance of a turbulent diffusion coefficient. For the ions, however, the linearized Vlasov response is sufficiently accurate. (The effect of turbulent diffusion is to smooth out the structure of the response functions over a scale length x_c . Since the ion response functions are characterized by a scale length x_i , satisfying $x_i > x_c$, the turbulent diffusion has no appreciable effect on the ion response.) These responses are then combined along with Ampere's Law and Quasineutrality to yield a coupled, self-adjoint system for the electric and magnetic fluctuation potentials.

A. Electron Response

The major goal here is to develop a model which includes the effects of turbulent electron diffusion in a self-consistent manner. In the NSA formalism, the lifetime of the long-scale potential fluctuations of the waves, τ_{ac} , is assumed to be long compared to the Kolmogorov time, τ_k , characterizing the rate of the randomization in the particle orbits. The amplitude of the wave fluctuations must be sufficiently large such that the phase-space islands overlap, thus, producing stochastic particle orbits. For example, in the case of drift waves, the island overlap condition is satisfied for very small fluctuation amplitudes. Hence, it is the drift waves themselves that produce the stochastic electron behavior and thus lead to turbulent diffusion. Using the NSA, this phenomenon of stochastic electron behavior is implemented in the stability analysis for the drift wave via a turbulent diffusion coefficient. In particular, one can show that the drift wave is unstable for very small values of the diffusion coefficient and then saturates at some finite value. In fact, it is possible to calculate the saturation value of the diffusion coefficient at which the drift wave stabilizes¹¹.

In the case of the tearing mode, the tearing mode itself will not (in cases of interest) produce island overlap and lead to stochastic electron behavior. To correctly account for turbulent electron behavior in this case, one must consider the tearing mode as existing among a background of turbulence such as that produced by finite-beta drift waves. Due to the large discrepancy in the poloidal wave numbers, m , of the tearing mode and the drift waves, their respective stability analyses can be performed largely independently. This discrepancy in the wave numbers also allows a spatial averaging over the scale length of the drift waves while keeping the tearing mode potentials fixed. (This averaging is unnecessary if the coarse-grain averaging of the stochastic particle orbits has been preformed.) The major effect of the drift waves on the tearing mode is that the electrons behave stochastically due to the presence of drift wave turbulence. This stochastic behavior manifests itself as a turbulent diffusion coefficient whose value is independent of the presence of the tearing mode. Hence, in the tearing mode analysis, the electron diffusion coefficient is treated as an independent external parameter, whose value is to be specified either by experimental observation or calculated through the use of an appropriate microturbulence theory for

drift waves.

The equation governing the perturbed electron distribution function, \tilde{f}_e , is the drift kinetic equation which when written for the fluctuations takes on the following form.

$$\begin{aligned}
& \left[\frac{\partial}{\partial t} + v_{\parallel} \mathbf{b} \cdot \nabla - \frac{c}{B} \nabla \left(\tilde{\phi} - \frac{v_{\parallel}}{c} \tilde{A}_{\parallel} \right) \times \mathbf{b} \cdot \nabla - \frac{e}{m} \tilde{\mathbf{E}} \cdot \mathbf{b} \frac{\partial}{\partial v_{\parallel}} \right] \tilde{f}_e \\
& = \left[\frac{c}{B} \nabla \left(\tilde{\phi} - \frac{v_{\parallel}}{c} \tilde{A}_{\parallel} \right) \times \mathbf{b} \cdot \nabla + \frac{e}{m} \tilde{\mathbf{E}} \cdot \mathbf{b} \frac{\partial}{\partial v_{\parallel}} \right] \bar{f}_e \\
& \equiv S_0(x)
\end{aligned} \tag{1}$$

Throughout the following, a tilde is used to denote fluctuation quantities. Here, $\tilde{\phi}$ and \tilde{A}_{\parallel} represent the perturbed electric and magnetic potentials respectively, $\tilde{\mathbf{E}}$ represents the perturbed electric field, and \bar{f}_e represents the equilibrium electron distribution function. The effects of the equilibrium electric field are represented by letting \bar{f}_e contain the equilibrium plasma current produced by this electric field.

For this problem a sheared, slab geometry is chosen with the equilibrium magnetic field given by $\mathbf{B} = B(\mathbf{e}_z + x/L_s \mathbf{e}_y)$ with $\mathbf{b} = \mathbf{B}/B$. Here, $L_s = -Rq^2/rq'$ is the shear length, and $x = 0$ is chosen to be the position of the rational surface. It will be shown that this model reduces to ideal MHD away from the rational surface. Because of this reduction to ideal MHD at large x , the following results for the tearing mode can be generalized quite easily to more complicated geometries simply by calculating the function Δ' for those geometries.

In the case of the tearing mode, the equilibrium plasma current is included in the electron distribution by writing $\bar{f}_e = f_0 + f_1$ where $f_0 = n_0/(\sqrt{\pi}v_e) \exp(-v_{\parallel}^2/v_e^2)$ and $f_1 = (2v_D v_{\parallel}/v_e^2) f_0$. Here, f_1 denotes a drifted Maxwellian (v_D is the drift speed) and is used to model the equilibrium current distribution.

Only a short summary of the basic principles and results of the NSA is presented here. A more detailed development of the NSA will appear later in a paper discussing the finite- β drift wave. Physically, the applicability of the NSA makes use of the observation that for sufficiently long times, $t > \tau_k$ ($\tau_k =$ Kolmogorov time for entropy production), the exact particle orbit perturbations, $\delta\theta(t)$, exhibit stochastic behavior. That is, for $t > \tau_k$ the

orbits $\delta\theta(\mathbf{x}, t)$ develop pathological spatial structure leading to sharp spatial gradients. In particular, orbits with neighboring initial data separate exponentially with time. The NSA makes use of the property that such stochastic orbits are characterized by an extremely fine spatial structure, much finer than the spatial structure of the corresponding fluctuation potentials, $\tilde{\phi}$ and \tilde{A}_{\parallel} . The wave lengths characterizing the fluctuations in the orbits δr and $\delta\theta$ are much shorter than those characterizing the potentials $\tilde{\phi}$ and \tilde{A}_{\parallel} . This allows \tilde{A}_{\parallel} and $\tilde{\phi}$ to be approximated as constants over a distance in which there occur many fluctuations in $\delta\theta$ and δr . The statistics of the orbits and the waves then become essentially independent, thus enabling a spatial averaging to be performed on the orbits over a distance in which the wave potentials do not exhibit random behavior.

The above argument implicitly assumes that $\tau_k \ll \tau_{ac}$, where τ_{ac} = the autocorrelation time for the fluctuation potential. When this is satisfied, the orbit functions exhibit random behavior on a time scale (represented by τ_k) much shorter than the time scale on which the fluctuation potentials randomize (represented by τ_{ac}). Typical estimates for the autocorrelation time is one over the real frequency of the mode, $\tau_{ac} \sim \omega_{*e}^{-1}$. In this model¹², the electron orbits exhibit diffusive behavior on the time scale $\tau_k \sim \omega_c^{-1}$, where $\omega_c^3 = (k'_{\parallel} v_e)^2 D/3$. For the $m = 2$ tearing mode, $\omega_c/\omega_{*e} \sim 10$, and hence $\tau_k < \tau_{ac}$. This procedure of performing a statistical average over the fine microscale of the orbits while holding the statistics of the waves fixed is known as “coarse graining”¹². (Note, for the case of drift waves, typically $\tau_{ac} \sim \tau_k$, and the validity of the NSA is more questionable than in the case of the tearing mode).

For short times, $t < t_k$, this procedure breaks down. On this short time scale, the electrons behave adiabatically. Hence, to correctly account for this short time behavior, the adiabatic piece of the perturbed electron distribution is first extracted before applying the NSA procedure. That is, one writes

$$\tilde{f}_e = \frac{e\tilde{\phi}}{T_e} f_o + \tilde{h}_e. \quad (2)$$

Inserting this into Eq. (1) yields the following equation for the nonlinear electron response, \tilde{h}_e .

$$\begin{aligned}
& \left[\frac{\partial}{\partial t} + v_{\parallel} \mathbf{b} \cdot \nabla - \frac{c}{B} \nabla \left(\tilde{\phi} - \frac{v_{\parallel}}{c} \tilde{A}_{\parallel} \right) \times \mathbf{b} \cdot \nabla - \frac{e}{m} \tilde{\mathbf{E}} \cdot \mathbf{b} \frac{\partial}{\partial v_{\parallel}} \right] \tilde{h}_e \\
& = \left[\frac{c}{B} \nabla \left(\tilde{\phi} - \frac{v_{\parallel}}{c} \tilde{A}_{\parallel} \right) \times \mathbf{b} \cdot \nabla (f_0 + f_1) \right. \\
& \quad \left. - \frac{e}{T_e} \frac{\partial}{\partial t} \left(\tilde{\phi} - \frac{v_{\parallel}}{c} \tilde{A}_{\parallel} \right) f_0 + \frac{e}{m} \tilde{\mathbf{E}} \cdot \mathbf{b} \frac{\partial}{\partial v_{\parallel}} f_1 \right] \\
& \equiv S(x)
\end{aligned} \tag{3}$$

where the terms inherently nonlinear in the fluctuation potentials have been neglected in the expression for $S(x)$. Only the nonlinear terms involving gradients of the perturbed distribution, \tilde{h}_e , are significant, since the gradients of \tilde{h}_e are characterized by much shorter wavelengths than those of the potentials $\tilde{\phi}$ and \tilde{A}_{\parallel} .

The nonlinear electron response, \tilde{h}_e , is given by applying the NSA to Eq. (3). In short, the NSA yields the following equation for the evolution of \tilde{h}_e .

$$\left(\frac{\partial}{\partial t} + v_{\parallel} \mathbf{b} \cdot \nabla - D \frac{\partial^2}{\partial x^2} \right) \tilde{h}_e = S(x) \tag{4}$$

In the above equation, D is the particle diffusion coefficient defined by $\langle \delta r(t)^2 \rangle \equiv 2Dt$ and is to be treated as a known constant in the solution of Eq. (4). Here $\delta r(t)$ represents the radial orbit perturbation due to random $\tilde{\mathbf{E}} \times B$ radial motion, such as that produced by turbulent drift waves, and the angular brackets are used to denote statistical averaging.

By comparing the above equation to Eq. (3), it is clear that the effect of applying the NSA to the drift kinetic equation is to convert the terms in the orbit operator (the left hand side of Eq. (3)) involving the fluctuation potentials into a spatial diffusion operator. This is a reflection of the physical assertion that the major contribution of these terms in the orbit operator is to produce stochastic orbits leading to turbulent spatial diffusion.

The nonlinear electron response, \tilde{h}_e , is given by solving Eq. (4) through the use of Fourier transforms. Defining the Fourier transform of $g(r, \theta, \phi, t)$ to be $g_k(r, m, n, \omega)$, then the nonlinear electron response is given by

$$\tilde{h}_{ek} = \int_0^{\infty} d\tau \int_{-\infty}^{\infty} dx' G(x, x'; v_{\parallel}, \tau) S_k(x'), \tag{5}$$

where the kernel $G(x, x'; v_{\parallel}, \tau)$ is given by

$$G(x, x'; v_{\parallel}, \tau) = \frac{1}{\sqrt{4\pi D\tau}} \exp \left[i(\omega - k'_{\parallel} v_{\parallel} x) \tau - \frac{1}{3} (k'_{\parallel} v_{\parallel})^2 D \tau^3 - \frac{1}{4D\tau} (x - x' - iDk'_{\parallel} v_{\parallel} \tau^2)^2 \right]. \quad (6)$$

Here $k_{\parallel} \equiv k'_{\parallel} x$, $k'_{\parallel} = k_y/L_s$ and $k_y = m/r$. Note that $G(x, x'; v_{\parallel}, \tau)$ decays with a characteristic time given by $\tau_c \equiv [(k'_{\parallel} v_e)^2 D/3]^{-1/3} \equiv \omega_c^{-1}$ and represents a peaked function of $x - x'$ with a characteristic width $x_c \equiv \omega_c/(k'_{\parallel} v_e)$.

In the case of the tearing mode, the drive term, $S(x)$, is given by the right hand side of Eq. (3). When the source terms, $S(x)$, appear in the combination $(\tilde{\phi} - (v_{\parallel}/c)\tilde{A}_{\parallel})$, then the coupled system obtained from quasineutrality and Ampere's Law is self-adjoint. The last source term in the above equation destroys this property. However, for the case of the tearing mode, this term can be dropped to give a self-adjoint system. This is due to the observation that the coupled equations obtained from Ampere's Law and Quasineutrality reduce to ideal MHD at large x (at large distances from the rational surface, $x = 0$), which implies $\tilde{E}_{\parallel} = 0$ at large x . At small x (inside the dissipative layer), the dissipative process of electron diffusion is insensitive to an equilibrium current.

Defining the resonant operators

$$R_n[\psi] = \int_{-\infty}^{\infty} dv_{\parallel} \int_{-\infty}^{\infty} dx' \int_0^{\infty} d\tau G(x, x'; v_{\parallel}, \tau) \left(\frac{v_{\parallel}}{v_e} \right)^n f_0(v_{\parallel}) \psi(x'), \quad (7)$$

then the perturbed electron density is given by

$$\frac{\tilde{n}_e}{n_0} = \frac{e}{T_e} \left\{ \tilde{\phi} + i[(\omega - \omega_{*e})R_0 - \omega_{*e}\eta_J R_1] \tilde{\phi} - i[(\omega - \omega_{*e})R_1 - \omega_{*e}\eta_J R_2] \frac{v_e}{c} \tilde{A}_{\parallel} \right\}, \quad (8)$$

and the perturbed parallel electron current is

$$\tilde{j}_{\parallel e} = \frac{-ie^2 n_0}{T_e} v_e \left\{ [(\omega - \omega_{*e})R_1 - \omega_{*e}\eta_J R_2] \tilde{\phi} - [(\omega - \omega_{*e})R_2 - \omega_{*e}\eta_J R_3] \frac{v_e}{c} \tilde{A}_{\parallel} \right\}, \quad (9)$$

where the appropriate velocity moments of \tilde{h}_e have been taken. In the above expressions, the following definitions were used:

$$\omega_{*e} \equiv \frac{ek_y T_e}{cBL_n}, \quad L_n \equiv \frac{-d \ln f_0}{dx} \quad \text{and} \quad \eta_J = \frac{v_e \partial f_1 / \partial x}{v_{\parallel} \partial f_0 / \partial x} = \frac{-2J'_{\parallel}}{env_e (\ln f_0)'}$$

Utilizing an appropriate ion response and applying Ampere's Law and Quasineutrality yields a coupled system for the potentials $\tilde{\phi}$ and \tilde{A}_{\parallel} .

B. Ion Response

The ion response is assumed to be "classical"; that is, the response is described by the linearized Vlasov equation. Although the island overlap condition is satisfied for the ions, the resulting turbulent diffusion has no appreciable effect on the ion response. The end result of turbulent diffusion is a smoothing of the structure of the response functions over a scale length x_c . Since the ion response is characterized by a scale length x_i satisfying $x_i > x_c$, the ion response virtually reduces to the linearized Vlasov response. For slab geometry with a density gradient in the x -direction, the linearized Vlasov equation is solved by using the standard techniques to yield \tilde{f}_i . From this, the perturbed density and current can be calculated by taking the appropriate parallel velocity moments.

$$\begin{aligned} \frac{\tilde{n}_i}{n_0} = -\frac{e}{T_i} \left\{ \tilde{\phi} + \frac{\omega - \omega_{*i}}{\omega} \left[\Gamma_0 \zeta Z(\zeta) \tilde{\phi} + (\Gamma_0 - \Gamma_1) \rho_i^2 \frac{d}{dx} \left(\zeta Z \frac{d\tilde{\phi}}{dx} \right) \right] \right. \\ \left. - \frac{\omega - \omega_{*i}}{\omega} \Gamma_0 \zeta (1 + \zeta Z) \frac{v_i}{c} \tilde{A}_{\parallel} \right\} \end{aligned} \quad (10)$$

and

$$\tilde{J}_{\parallel i} = -\frac{e^2 n_0 v_i}{\Gamma_i} \left\{ \frac{\omega - \omega_{*i}}{\omega} \zeta (1 + \zeta Z) \Gamma_0 \left(\tilde{\phi} - \frac{v_i}{c} \zeta \tilde{A}_{\parallel} \right) \right\} \quad (11)$$

In the above expressions, $Z(\zeta)$ is the plasma dispersion function with $\zeta = \omega / (|k_{\parallel}| v_i)$ and $\Gamma_n = \Gamma_n(b) = I_n(b) \exp(-b)$ where $I_n(b)$ is the modified Bessel function with $b = k_y^2 \rho_i^2$.

In deriving the above expression for the perturbed ion density, Eq. (10), the electric potential, $\tilde{\phi}(x')$, was expanded about $x' = x$ to second order thus yielding the second derivative term in Eq. (10). This expansion is only valid when $x/x_i < 1$, $x_i \equiv \omega/k'_{\parallel} v_i$.

Hence, in evaluating the above ion Z -functions, one should use the large argument expansions (for $\zeta > 1$).

C. Coupled Equations for $\tilde{\phi}$ and \tilde{A}_{\parallel}

Knowing the perturbed density and current for both the electrons and ions, a coupled system of equations for $\tilde{\phi}$ and \tilde{A}_{\parallel} can be formed by utilizing quasineutrality and Ampere's Law.

Quasineutrality states that $\tilde{n}_i = \tilde{n}_e$. Using Eqs. (8) and (10), then this implies

$$L_1 \tilde{\phi} + L_x \tilde{A}_{\parallel} = 0. \quad (12)$$

Utilizing the parallel component of Ampere's Law along with Eqs. (9) and (11) gives

$$L_2 \tilde{A}_{\parallel} + L_x \tilde{\phi} = 0. \quad (13)$$

In writing the above equations, the following shorthand notation has been used:

$$\begin{aligned} L_1 &= \left[\frac{d}{dx} \zeta Z \frac{d}{dx} + \Lambda + \chi^2 + \frac{i}{d} (\omega - \omega_{*e}) R_0 - \frac{i}{d} \omega_{*e} \eta_J R_1 \right] \\ L_2 &= \frac{\tau v_A^2}{dc^2} \left[\frac{d^2}{dx^2} - b + \alpha_i^2 + \frac{v_e^2}{\tau v_A^2} i (\omega - \omega_{*e}) R_2 - \frac{v_e^2}{\tau v_A^2} i \omega_{*e} \eta_J R_3 \right] \\ L_x &= - \left[\frac{i}{d} (\omega - \omega_{*e}) R_1 - \frac{i}{d} \omega_{*e} \eta_J R_2 + x_e \chi^2 \right] \frac{v_e}{c} \end{aligned}$$

along with the following definitions:

$$\begin{aligned} d &= (\Gamma_0 - \Gamma_1) \left(\tau + \frac{\omega_{*e}}{\omega} \right), \quad \tau = T_e / T_i, \\ \Lambda &= \frac{1}{d} \left(1 + \tau - \Gamma_0 \left(\tau + \frac{\omega_{*e}}{\omega} \right) \right), \\ \chi^2 &= \frac{\Gamma_0}{d} \left(\tau + \frac{\omega_{*e}}{\omega} \right) (1 + \zeta Z), \\ \alpha_i^2 &= \frac{v_i^2}{\tau v_A^2} \left(\tau + \frac{\omega_{*e}}{\omega} \right) \zeta^2 (1 + \zeta Z) \Gamma_0, \quad b = \rho_i^2 k_y^2, \end{aligned}$$

where $\zeta = \omega/(|k_{\parallel}|v_i)$, $x_e = \omega/(|k_{\parallel}|v_e)$, and $Z =$ plasma dispersion function. In the above expressions, R_n denote the electron resonance operators and are defined in Eq. (7) and x is normalized in units of the ion gyroradius, ρ_i .

The above system is a kinetic description globally valid over the entire plasma which reduces to ideal MHD at large distances from the rational surface (large x), and is self-adjoint. When analyzed for high m modes this system yields unstable finite- β drift waves, and when analyzed for low m modes this system yields the tearing mode.

Since the above system is self-adjoint, a variational principle can be formed. The variational integral, S , is obtained by

$$S = - \int_{-a}^a dx [\tilde{\phi} L_1 \tilde{\phi} + \tilde{A}_{\parallel} L_2 \tilde{A}_{\parallel} + 2\tilde{\phi} L_x \tilde{A}_{\parallel}], \quad (14)$$

such that variation of S with respect of $\tilde{\phi}$ and \tilde{A}_{\parallel} yields the coupled Eqs. (12) and (13). The variational parameters characterizing suitable trial functions, $\tilde{\phi}_T$ and $\tilde{A}_{\parallel T}$, are thus determined by requiring $\delta S = 0$. Once these variational parameters have been determined, the trial functions are again inserted into Eq. (14) and the dispersion relation for these trial functions is determined by setting $S = 0$. This variational principle will be utilized later in a calculation of the dispersion relation for the tearing mode.

III. Kinetic Tearing Mode

In this section, a variational calculation is presented starting from the coupled equations for $\tilde{\phi}$ and \tilde{A}_{\parallel} , Eqs. (12) and (13). This calculation will lead to a dispersion relation which includes the effects of a non-zero electrostatic potential, $\tilde{\phi}$, which was neglected previously in Ref. [8]. This non-zero $\tilde{\phi}$ will couple the tearing mode to the drift wave branch, Eq. (12), and will lead to important stabilizing terms, representing ion inertia, in the dispersion relation. (Recall that the basic magnetic tearing mode of Ref. [8] is described by $L_2\tilde{A}_{\parallel} = 0$, whereas the basic electrostatic drift mode is described by $L_1\tilde{\phi} = 0$.)

A. Resistive Tearing Mode Limit

In the above fully kinetic analysis, calculation of the nonlinear electron response led to the resonance operators, $R_n[\psi]$, as given by Eq. (7). In the limit that $\psi(x')$ is a slowly varying function of x' , that is, if $x_c/x_T < 1$, where $x_T^{-1} = |d/dx(\ln \psi)|$, then $\psi(x')$ can be expanded about $x' = x$. To leading order in x_c/x_T the above resonance operators can be replaced by multiplicative operators of the form $R_n[\psi] \simeq I_n(x)\psi(x)$, where

$$I_n(x) = \int_{-\infty}^{\infty} dv_{\parallel} \left(\frac{v_{\parallel}}{v_e} \right)^n f_0(v_{\parallel}) \int_0^{\infty} d\tau \exp \left[i(\omega - k'_{\parallel}v_{\parallel}x)\tau - \frac{1}{3}(k'_{\parallel}v_{\parallel})^2 D\tau^3 \right]. \quad (15)$$

The above multiplicative resonance functions can be evaluated asymptotically to yield the following interpolation functions¹³.

$$\begin{aligned} I_0 &\simeq \frac{2.8}{\omega_c} \left[1 + 1.58 \left(\frac{x}{x_c} \right)^2 \right]^{-1} \\ I_2 &\simeq \frac{.47}{\omega_c} \left[1 + \left(\frac{x}{x_c} \right)^2 \right]^{-1} \\ I_1 &\simeq \frac{-.29i}{\omega_c} \frac{x}{x_c} \left[1 + .29 \left(\frac{x}{x_c} \right)^2 \right]^{-1} \\ I_3 &\simeq \frac{-.24i}{\omega_c} \frac{x}{x_c} \left[1 + .48 \left(\frac{x}{x_c} \right)^2 \right]^{-1} \end{aligned} \quad (16)$$

The above asymptotic behavior can be reproduced qualitatively if the exponential in Eq. (15) involving the factor $-1/3(k'_{\parallel}v_{\parallel})^2 D\tau^3 \simeq -\omega_c^3 \tau^3$ is replaced by the linear factor $-.36\omega_c \tau$. Under this approximation, the above resonance functions, $I_n(x)$, can be evaluated exactly in terms of the Z -function. This approximation will be referred to as the Krook limit.

$$\begin{aligned} I_n(x)_{krook} &= \int_{-\infty}^{\infty} dv_{\parallel} \left(\frac{v_{\parallel}}{v_e} \right)^n f_0(v_{\parallel}) \int_0^{\infty} d\tau \exp[i(\omega - k'_{\parallel}v_{\parallel}x)\tau - .36\omega_c \tau] \\ &= \int_{-\infty}^{\infty} dv_{\parallel} \left(\frac{v_{\parallel}}{v_e} \right)^n \frac{if_0(v_{\parallel})}{\omega_0 - k'_{\parallel}v_{\parallel}x} \end{aligned} \quad (17)$$

where $\omega_0 = \omega + i0.36\omega_c$. These integrals can be evaluated in terms of the Z -functions. Essentially, under the Krook approximation the turbulent spatial diffusion operator in Eq. (4), $-D\partial^2/\partial x^2$, is replaced by a krook type diffusion frequency, $0.36\omega_c$.

The resistive limit can be obtained by replacing ω_c with a collision frequency, ν . If this is done, along with setting the particle drift frequencies to zero, $\omega_* = 0$, while letting the dissipative layer become infinitesimally thin in the calculation of the energy drive, Δ' , then the resistive MHD result for the growth rate³ is reproduced.

B. Proof of Stability for Large Turbulent Diffusion

From previous theories of the resistive tearing mode³, the available magnetic energy of the outer ideal MHD region, represented by Δ'_0 , drives the tearing mode unstable. (A detailed study of the magnetic energy drive is given by Adler et al.¹⁴). In light of this, a general energy drive for the tearing mode is then defined to be the negative energy from the integral

$$S = \int_{-a}^a dx \left[A_{\parallel}^{\prime 2} + k_y^2 A_{\parallel}^2 + \frac{4\pi}{c} \tilde{J}_{\parallel e}[A_{\parallel}] \cdot A_{\parallel} \right] \quad (18)$$

where $\tilde{J}_{\parallel e}$ is the full kinetic operator representing the perturbed parallel current,

$$\frac{4\pi}{c} \tilde{J}_{\parallel e}[A_{\parallel}] = \frac{v_e^2}{\tau v_A^2} i\eta_J \omega_{*e} R_3[A_{\parallel}].$$

Hence, $S < 0$ is a necessary condition for instability.

In the resistive MHD limit, $R_3 = -i/2k_{\parallel}v_e$, and the negative energy drive takes on the ideal MHD form as indicated by the expression $S_{resistive} = -A_{\parallel 0}^2 \Delta'_0$, where $\lim_{x_0 \rightarrow 0} [A_{\parallel} A'_{\parallel}(x_0) - A_{\parallel} A'_{\parallel}(-x_0)]_{MHD} \equiv A_{\parallel 0}^2 \Delta'_0$ and $A_{\parallel}(x_0 \pm) \equiv A_{\parallel 0}$. Here, $A_{\parallel MHD}$ is defined to be the solution to the following equation,

$$\left[\frac{d^2}{dx^2} - k_y^2 - \frac{4\pi k_y J'_{\parallel}}{c k_{\parallel} B_0} \right] \tilde{A}_{\parallel} = 0, \quad (19)$$

which is the equation for marginal stability in ideal MHD. Δ'_0 represents the jump in \tilde{A}'_{\parallel} across the singular surface (for nearly constant A_{\parallel} or the “constant ψ ” approximation). Hence, in resistive MHD, Δ'_0 represents the available magnetic energy to drive the tearing mode. Instability is then obtained when $\Delta'_0 > 0$. (In the limit of large x , $x \gg x_c$, the MHD limit, $R_3 = -i/2k_{\parallel}v_e$, is also obtained in the fully kinetic description.)

Notice that in the energy integral given by Eq. (18), the first two terms are stabilizing and it is only the third term involving the perturbed current operator which can be negative and thus drive the tearing mode unstable. In the resistive MHD treatment, the perturbed current operator is singular at the rational surface. In fact, it is this singular behavior which dominates in the integral S and typically causes Δ'_0 to be positive (and hence S to be negative). However, if one retains the full kinetic operator for $\tilde{J}_{\parallel e}[A_{\parallel}]$ involving the resonance operator $R_3[A_{\parallel}]$, then this operator is no longer singular at $x = 0$. In fact, one can easily show that the integral

$$S_J \equiv \int_{-a}^a dx \frac{4\pi}{c} \tilde{J}_{\parallel e}[\tilde{A}_{\parallel}] A_{\parallel} \quad (20)$$

is bounded for $D > 0$. Not only this, but one can also show that $|S_J| \rightarrow 0$ as $D \rightarrow \infty$. Hence, the conclusion is reached that for some critical value of the diffusion coefficient, $D = D_{cr}$, the energy drive, S , will be zero and the tearing mode is stabilized.

C. Variational Calculation

A detailed calculation of the dispersion relation is now presented, including the effects of the electrostatic coupling terms. This is done through the use of a variational principle. The starting point is again Ampere's Law and Quasineutrality, given by Eqs. (12) and (13). To leading order in ω_*/ω_c , the effects of the resonant operators can be neglected in the electrostatic operator, L_1 , and the coupling operator, L_x .

$$L_1 \simeq \left[\frac{d}{dx} \zeta Z(\zeta) \frac{d}{dx} + \Lambda + \chi^2 \right], \quad L_x \simeq -\frac{v_e}{c} x_e \chi^2 \quad (21)$$

The expansion used to yield the differential operator in the expression for L_1 implicitly assumed that $|x/x_i| < 1$, that is, $\zeta > 1$. Using the above approximations and expanding the ion Z -functions for large arguments, quasineutrality can then be written as

$$\left[-\frac{d^2}{dx^2} + \Lambda - \frac{1}{2} \frac{x^2}{x_i^2} \right] \tilde{\phi} + \frac{1}{2} \frac{x^2}{x_i^2} \frac{\omega}{k_{\parallel} c} \tilde{A}_{\parallel} \simeq \mathcal{O}\left(\frac{\omega_*^2}{\omega_c^2}\right) \quad (22)$$

where $x_i = \omega/(k_{\parallel}' \rho_i v_i)$. Scaling $\omega_*/\omega_c \sim \epsilon$, $\omega/\omega_* \sim 1$, $x^2/x_i^2 \sim \epsilon$ and $d^2/dx^2 \sim \epsilon^2$, then, for large x , $x/x_c > 1$, quasineutrality implies to leading order, $\Lambda \simeq 0 \rightarrow \omega \simeq \omega_{*e}$, and to first order in ϵ quasineutrality implies $\tilde{E}_{\parallel} = 0$. Thus, in the outer region, the equation for quasineutrality requires $\omega \simeq \omega_{*e}$ and reduces to the ideal MHD constraint $\tilde{E}_{\parallel} \simeq 0$. Also at large x , $|x/x_c| > 1$, assuming $\tilde{E}_{\parallel} = 0$, Ampere's Law reduces to the ideal MHD equation of marginal stability, given by Eq. (19). Hence, the coupled Eqs. (12) and (13) reduce to ideal MHD with the additional constraint that $\omega \simeq \omega_{*e}$ in the outer region where $|x| > x_c$.

Since the equations governing \tilde{A}_{\parallel} and $\tilde{\phi}$ are self-adjoint, a simple variational integral, Eq. (14), is obtained. In this calculation, $\pm a$ represents the edges of an intermediate integration region which is assumed to lie in the region where ideal MHD is approximately valid (that is, $a > x_c$).

Integrating by parts, Eq. (14) becomes

$$S = \frac{\tau v_A^2}{dc^2} [\mathcal{L}_A - \beta_A] + [\mathcal{L}_{\phi} - \beta_{\phi}] \quad (23)$$

where

$$\mathcal{L}_\phi = \int_{-a}^a dx \left[\zeta Z \left(\frac{d\tilde{\phi}}{dx} \right)^2 - \Lambda \tilde{\phi}^2 - \frac{\Gamma_0}{d} \left(\tau + \frac{\omega_{*e}}{\omega} \right) (1 - \zeta Z) \left(\tilde{\phi} - \frac{\omega}{k_{\parallel} c} \tilde{A}_{\parallel} \right)^2 \right] \quad (24)$$

$$\mathcal{L}_A = \int_{-a}^a dx \left[\left(\frac{d\tilde{A}_{\parallel}}{dx} \right)^2 + \left(b - \frac{v_e^2}{\tau v_A^2} i(\omega - \omega_{*e}) R_2 + \frac{v_e^2}{\tau v_A^2} i\omega_{*e} \eta_J R_3 \right) \tilde{A}_{\parallel}^2 \right] \quad (25)$$

$$\beta_\phi = \zeta Z \tilde{\phi} \tilde{\phi}' \Big|_{-a}^a \quad \text{and} \quad \beta_A = \tilde{A}_{\parallel} \tilde{A}'_{\parallel} \Big|_{-a}^a$$

Here, \mathcal{L}_A represents the contribution of the magnetic terms (involving the electron response only) with the corresponding boundary terms β_A . The contributions of the electrostatic, coupling and the ion terms are represented by \mathcal{L}_ϕ with the boundary terms β_ϕ . The magnetic tearing mode considered above in Part B is accounted for in the \mathcal{L}_A and β_A terms. That is,

$$\mathcal{L}_A - \beta_A = \int_{-a}^a dx \tilde{A}_{\parallel} L_2 \tilde{A}_{\parallel} \quad (26)$$

where it has been shown above that $L_2 \tilde{A}_{\parallel} = 0$ yields the basic collisionless magnetic tearing mode. Hence, \mathcal{L}_ϕ and β_ϕ represent the contributions to the dispersion relation which are due to coupling to the electrostatic branch as well as the ion contributions to the perturbed current.

At the boundary, $\pm a$, \tilde{A}_{\parallel} and $\tilde{\phi}$ are required to match onto the ideal MHD solution. In particular, at the boundary, $\tilde{E}_{\parallel} = 0$. Using this condition, the magnitude of the boundary terms β_ϕ and β_A can be compared. Noting $\beta_\phi \sim (\omega/k_{\parallel} c)^2 \tilde{A}_{\parallel} \tilde{A}'_{\parallel}$, then it is easy to show that the contribution of β_ϕ to the dispersion relation is smaller than that of β_A by ω_*^2/ω_c^2 . Hence, the boundary term β_ϕ can be neglected.

The above variational integral will be performed using two steps. First, the electrostatic integral will be calculated using a suitable trial function for $\tilde{\phi}$ while assuming \tilde{A}_{\parallel} to be a constant in the $\tilde{\phi} - (\omega/k_{\parallel} c) \tilde{A}_{\parallel}$ term (which is justified by the fact that \tilde{A}_{\parallel} is nearly constant while $\tilde{\phi}$ must be linear in x near the rational surface). One can then solve for $\tilde{\phi}$ variationally. After this, the magnetic terms $\mathcal{L}_A - \beta_A$ are calculated using a linear trial function for \tilde{A}_{\parallel} while allowing the limit of integration, a , to be the variational parameter.

The electrostatic integral, \mathcal{L}_ϕ , is given by Eq. (24). In the above expression, one must keep in mind that the ion Z -functions are to be expanded for large arguments. Here, Λ represents the eigenfrequency and is approximately zero when $\omega \simeq \omega_{*e}$ and, hence, will be neglected. The first term in Eq. (24) represents the $\tilde{\mathbf{E}} \times \mathbf{B}$ ion motion in the poloidal direction whereas the last term represents the ion motion along the field lines.

A trial function of the following form is chosen

$$\tilde{\phi} = \frac{\omega}{k'_{\parallel} c} A_0 \frac{x}{(x^2 \pm i\alpha^2)}, \quad A_0 \equiv \text{constant}. \quad (27)$$

Here, α is the variational parameter and it is assumed $(\alpha/a)^2 \ll 1$ such that at the boundary, $x = a$, one has $\tilde{E}_{\parallel} \simeq 0$. Hence, Eq. (24) becomes

$$\mathcal{L}_\phi = \left(\frac{\omega}{k'_{\parallel} c} \right)^2 A_0^2 \int_{-a}^a dx \left[\zeta Z \frac{(\pm i\alpha^2 - x^2)^2}{(\pm i\alpha^2 + x^2)^4} + \frac{(1 + \zeta Z)}{x^2} \frac{\alpha^2}{(\pm i\alpha^2 + x^2)^2} \right]. \quad (28)$$

Using the large argument expansions for the Z -functions along with the variable substitution $y = x/\alpha$ and assuming $a/\alpha \gg 1$, then the limits of integration can be extended to infinity. These integrals can be evaluated explicitly to give the expression

$$\mathcal{L}_\phi \simeq \left(\frac{\omega}{k'_{\parallel} c} \right)^2 A_0^2 \frac{\sqrt{2}}{8} \pi (1 \pm i) \left[\frac{1}{\alpha^3} + \frac{\alpha}{x_i^2} \right]. \quad (29)$$

The variational parameter is then specified according to $\delta \mathcal{L}_\phi / \delta \alpha = 0$ which yields $\alpha^2 = \sqrt{3} x_i = \sqrt{3} \omega / (k'_{\parallel} v_i \rho_i)$. Inserting this expression for α^2 back into Eq. (29) then gives

$$\mathcal{L}_\phi \simeq \frac{\pi}{\sqrt{2} 3^{3/4}} A_0^2 \left(\frac{v_i}{c} \right)^{3/2} \left(\frac{\omega}{k'_{\parallel} \rho_i c} \right)^{1/2} (1 \pm i). \quad (30)$$

Note that this expression is independent of a , which serves as the variational parameter in the calculation of the magnetic integrals.

The magnetic contributions to the variational form, S , are now calculated. The magnetic terms are given by Eq. (25) with the boundary term β_A . Assuming $x_c < [d \ln A / dx]^{-1}$, then one can approximate the resonance operators, R_n , by the multiplicative operators, I_n , as given in Eq. (15). Thus

$$\mathcal{L}_A - \beta_A \simeq \int_{-a}^a dx \left[A'^2 + \left(b + \frac{\Gamma}{\omega_c} \frac{1}{1 + (\frac{x}{x_c})^2} + \frac{\lambda x}{2 x_c^2} \frac{1}{1 + \frac{1}{2}(\frac{x}{x_c})^2} \right) A^2 \right] - AA' \Big|_{-a}^a \quad (31)$$

where $\Gamma = -i(v_e^2/\tau v_A^2)(\omega - \omega_{*e})$ and $\lambda = .5(v_e^2/\tau v_A^2)(\omega_{*e}/\omega_c)\eta_J x_c$.

For the trial functions, the following forms are used. In the outer region, $|x| > a$, $A_{||}$ is required to be the ideal MHD solution. That is, $A_{||} = A_{MHD}$ for $|x| > a$, where A_{MHD} must solve Eq. (19). To leading order for small x/x_J , where $x_J^{-1} \equiv |d/dx(\ln J_{||})|$, Eq. (19) can be solved asymptotically to yield

$$A = \begin{cases} A_+^{MHD} = f + C_+ g & \text{for } x > a \\ A_-^{MHD} = f + C_- g & \text{for } x < -a \end{cases} \quad (32)$$

where

$$\begin{aligned} f &\simeq 1 + \frac{\lambda x}{2} \ln x^2 + \frac{\lambda^2 x^2}{4} (\ln x^2 + 2b - 3) + \dots \\ f' &\simeq \frac{\lambda}{2} [\ln x^2 + 2] + \frac{\lambda^2 x}{2} [\ln x^2 + 2b - 2] + \dots \\ g &\simeq \lambda x + \frac{\lambda^2 x^2}{2} + \dots, \quad g' \simeq \lambda + \lambda^2 x + \dots \end{aligned} \quad (33)$$

and it is assumed $\lambda x \sim \lambda a \ll 1$.

Consider the following definition, $\Delta'(x) \equiv A'_{+MHD} - A'_{-MHD}$. Numerical calculations for Alcator C parameters⁷ indicate $\Delta'(x)$ to be primarily a linear function of x of the form $\Delta'(x) = \Delta_0(1 - x/W)$. Here, W represents the nonlinear island saturation width¹⁵. Hence, by identifying

$$C_+ - C_- = \Delta_0/\lambda; \quad C_+ + C_- = \frac{-\Delta_0}{\lambda^2 W} \quad (34)$$

and by requiring $\lambda^2 a C_{\pm} > \lambda^2 a$, then to leading order, $\Delta'(x) \simeq \Delta_0(1 - x/W)$. For the sake of simplicity in the following calculations, the following approximate forms are used as definitions.

$$\begin{aligned}
f &\equiv 1 + \lambda x, & g &\equiv \lambda x + \frac{\lambda^2 x^2}{2} \\
f' &\equiv \lambda, & g' &\equiv \lambda + \lambda^2 x
\end{aligned}
\tag{35}$$

By doing this, then one directly obtains the desired result that $\Delta'(x) = \Delta_0(1 - x/W)$. Strictly speaking, however, the forms of f and g used in Eq. (35) are only approximately valid when $C_{\pm} > 1$. This constraint can be relaxed, however, if the forms in Eq. (51) are taken to define the outer trial functions for $|x| > a$. In any event, requiring $A_{MHD} > 0$ (as is indicated from experimental profiles) implies the restraint $\lambda a C_{\pm} < 1$. Utilizing the scaling $C_{\pm} \sim \Delta_0/(\lambda^2 W)$, then requiring $A_{MHD} > 0$ implies $\Delta_0 a/(\lambda W) < 1$.

The trial function for the inner region is taken to be a slowly varying linear function of x .

$$A = \begin{cases} A_+ = 1 + L_+ x & \text{for } 0 < x < a \\ A_- = 1 + L_- x & \text{for } -a < x < 0 \end{cases}
\tag{36}$$

Requiring this trial function to be continuous at the boundary, $x = \pm a$, with the ideal MHD solution then defines L_{\pm} to be

$$L_{\pm} = \lambda + C_{\pm} \lambda \left(1 \pm \frac{\lambda a}{2} \right).
\tag{37}$$

Using these trial functions, it is now possible to evaluate the magnetic form $\mathcal{L}_A - \beta_A$. The boundary terms are given by

$$\begin{aligned}
\beta_A &\equiv AA' \Big|_{-a}^a = A_+ A'_{+MHD} \Big|_a - A_- A'_{-MHD} \Big|_{-a} \\
&= \Delta'(a) + a(L_+^2 + L_-^2) + \frac{\lambda^2 a^2}{2} (L_+ C_+ - L_- C_-)
\end{aligned}
\tag{38}$$

where $\Delta'(a) = \Delta_0(1 - a/W)$.

In the magnetic variational terms, $S_A = \mathcal{L}_A - \beta_A$, the variational parameter is chosen to be the limit of integration, a , which also characterizes the slope of the trial function.

Note that the electrostatic term, \mathcal{L}_ϕ , was evaluated approximately to be independent of a . Thus, only the magnetic terms determine the variational parameter a .

Variation of the magnetic form, S_A , with respect to a then gives

$$\frac{\delta S_A}{\delta a} = \left[A'^2 + \left(b + \frac{\Gamma}{\omega_c} \frac{1}{1 + (\frac{x}{x_c})^2} + \frac{\lambda x}{2 x_c^2} \frac{1}{1 + \frac{1}{2}(\frac{x}{x_c})^2} \right) A^2 \right] \Big|_{+a} - \Big|_{-a} - \frac{\delta \beta_A}{\delta a}. \quad (39)$$

Recall that requiring $A_\pm > 0$ leads to the constraint $L_\pm a < 1$. Also, in the evaluation of the boundary term, it suffices to approximate L_\pm as independent of a ; that is, $L_\pm \simeq C_\pm \lambda$. Hence, to leading order in $L_\pm a$,

$$\frac{\delta S_A}{\delta a} = \frac{\Delta_0}{W} + 2b + \frac{2\Gamma}{\omega_c} \frac{1}{1 + (\frac{a}{x_c})^2} - \lambda \frac{a^2}{x_c^2} \frac{1}{1 + \frac{1}{2}(\frac{a}{x_c})^2} \frac{\Delta_0}{\lambda W}. \quad (40)$$

Typically, $b \sim \lambda^2$, and $\Delta_0 \sim \lambda$. Thus, $bW/\Delta_0 \sim \lambda a \ll 1$, and the second term in the above equation can be ignored. Assuming $\omega = \omega_{*e} + i\gamma$, then at marginal stability, $\Gamma \simeq 0$. Setting $\delta S_A/\delta a = 0$ and solving for a yields $a^2 \simeq 2x_c^2$.

To find the dispersion relation, the integral form S_A is evaluated explicitly. From Eq. (31),

$$\begin{aligned} S_A = & \left[a(L_+^2 + L_-^2) + 2ba + 2 \frac{\Gamma}{\omega_c} \left(\tan^{-1} \frac{a}{x_c} \right) x_c \frac{a}{\sqrt{2x_c}} \right. \\ & \left. + 2\lambda x_c (L_+ + L_-) \left(\frac{a}{x_c} - \sqrt{2} \tan^{-1} \frac{a}{\sqrt{2x_c}} \right) \right] \\ & - [\Delta'(a) - (L_+^2 + L_-^2)a]. \end{aligned} \quad (41)$$

Approximating $L_+ + L_- \simeq -\Delta_0/\lambda W$ and using the result $a \simeq \sqrt{2x_c}$ along with the definition $\Delta'(\sqrt{2x_c}) = \Delta_0(1 - \sqrt{2x_c}/W)$ then gives

$$S_A \simeq -\Delta' \left(\frac{\sqrt{2}}{2} x_c \right) + 2\sqrt{2} b x_c + \frac{2\Gamma}{\omega_c} x_c. \quad (42)$$

The overall dispersion relation including the electrostatic terms is given by Eq. (23). Using the results of Eqs. (25) and (42) gives the following dispersion relation

$$\frac{2\Gamma}{\omega_c} x_c = \Delta' \left(\frac{\sqrt{2}}{2} x_c \right) - 2\sqrt{2} x b_c - \frac{d}{\tau} \left(\frac{v_i}{v_A} \right)^2 \left(\frac{\omega}{k'_{\parallel} \rho_i v_i} \right)^{1/2} (1 \pm i). \quad (43)$$

The above expression is valid provided $bW/\Delta_0 < 1$ and $\Delta_0 a/\lambda W < 1$. On the right hand side of Eq. (43), one can approximate $\omega \simeq \omega_{*e}$, $d \simeq 2$, and $\tau = 1$. Recalling the definition of Γ and letting $\omega = \omega_R + i\gamma$ with $|\gamma/\omega_R| \ll 1$, then gives a real frequency

$$\omega_R = \omega_{*e} \pm \frac{v_i}{v_e} \left(\frac{L_n}{L_s} \right)^{1/2} \omega_{*e} \quad (44)$$

and a growth rate given by

$$\gamma = \frac{k'_{\parallel} \rho_i v_e}{2} \left\{ \frac{v_A^2}{v_e^2} \left[\Delta' \left(\frac{\sqrt{2}}{2} x_c \right) - 2\sqrt{2} b x_c \right] - 2 \left(\frac{L_s}{L_n} \right)^{1/2} \left(\frac{v_i}{v_e} \right)^2 \right\}. \quad (45)$$

In the limit $bW/\Delta_0 \ll 1$, then stability is obtained when $\gamma < 0$, or

$$x_c > \sqrt{2} W \left[1 - \frac{2}{\Delta_0} \beta_i \left(\frac{L_s}{L_n} \frac{\tau}{\sqrt{2}} \right)^{1/2} \right]. \quad (46)$$

Thus, it is apparent that the coupling to the electrostatic branch, represented by the second term on the right of Eq. (46) is a stabilizing effect. Physically, this term represents that fraction of the available energy which is necessary to maintain the ion motion.

The first term on the right in the expression for the growth rate, Eq. (45), represents the magnetic energy drive from the ideal MHD region. Recall, $\Delta'(x) \simeq \Delta_0(1-x/W)$, where W corresponds to the island saturation width of resistive MHD. Hence, the tearing mode will be stabilized if $\Delta'(x_c) < 0$ or $x_c > W$. Since $x_c \sim D^{1/3}$, this implies that if $D \sim 1/n$, then there exists a density threshold which must be surpassed before instability occurs. Physically, $\Delta'(x_c)$ is interpreted as the magnetic energy in the outer region available to drive the tearing mode. In essence, the turbulent electron diffusion prohibits the formation of, or flattens, the perturbed parallel current, $\tilde{J}_{\parallel e}$, within a finite correlation distance, x_c , of the rational surface. This has the effect of reducing the available magnetic energy drive from the value $\Delta'(0)$ to $\Delta'(x_c)$. The second term on the right of Eq. (45) represents line bending in the inner dissipative region and is stabilizing. The last term is ion inertia stabilization, and represents that portion of energy necessary to sustain the ion oscillation at frequency ω_* .

IV. Numerical Results

This section presents numerical solutions of the eigenmodes and eigenfrequency for the tearing mode. The equations governing the evolution of perturbed particle densities, \tilde{f}_e and \tilde{f}_i , are solved numerically and through the aid of Ampere's Law and Quasineutrality the eigenmodes, $\tilde{\phi}$ and \tilde{A}_{\parallel} , along with the eigenfrequency, ω , are calculated. Two numerical codes are employed in this calculation of the eigenfrequency for two different limits. The first method, which is the more exact method, involves the use of an initial value code, TEDIT¹³, previously used in the study of the finite beta drift wave. Specifically, TEDIT solves for the electron response utilizing the full diffusion operator, $D\partial^2/\partial x^2$. The second method involves a shooting code, inherently simpler than the initial value code, which solves for the electron response in the Krook approximation: Both codes give qualitatively similar results and support the above analytical expression for the dispersion relation arrived at through the variational calculation.

The initial value code, TEDIT, follows the time evolution of all the perturbed quantities. One begins with arbitrary perturbed potentials, $\tilde{\phi}$ and \tilde{A}_{\parallel} , and distribution functions, \tilde{f}_e and \tilde{f}_i . Regardless of the initial functions, if a growing (unstable) eigenmode exists, it will eventually dominate the long time solution. By definition, an eigenmode exists when all quantities $\tilde{\phi}$, \tilde{A}_{\parallel} , \tilde{f}_e and \tilde{f}_i vary as $\exp(-i\omega t)$, where the eigenfrequency ω is constant for all x . The main virtue of this initial value approach is that it allows for the electron response to be evolved with the inclusion of a spatial diffusion operator according to Eq. (4) of Sec. II. The ion response evolves according to the linearized Vlasov equation. The time-evolution code TEDIT uses an implicit-iterative scheme to advance the electron and ion kinetic equations in time, with $\tilde{\phi}$ and \tilde{A}_{\parallel} being calculated from the quasineutrality condition and Ampere's Law. The equations for the electron and ion responses are advanced in time until

$$\omega(x, t) = \frac{i}{A_{\parallel}(x, t)} \frac{\partial A_{\parallel}(x, t)}{\partial t} \quad (47)$$

becomes independent of both x and t , indicating that an eigenmode of frequency ω has been established. For a given set of parameters, TEDIT yields the most unstable eigenmode.

In the Krook approximation, a shooting code is employed to solve for the eigenfrequency in the case where the electron response evolves according to Eq. (4) with $-D\partial^2/\partial x^2$ replaced with a Krook type diffusion frequency, ω_c . As discussed above in Sec. III, this is analytically shown to be valid when $x_c/x_T < 1$, and when \tilde{A}_{\parallel} is approximately a constant (an even function) near the rational surface. Under this approximation, a shooting code can be used to directly solve the coupled equations for $\tilde{\phi}$ and \tilde{A}_{\parallel} , given by Eqs. (12) and (13) in Sec. II. In this case, the resonance operators appearing in L_1 , L_2 and L_x can be written in terms of the plasma dispersion function as discussed in Sec. III. The above coupled equations can then be solved using standard shooting methods which is inherently simpler numerically than the initial value method used in the time-evolving code TEDIT.

In either case, the above numerical codes are used to calculate the eigenfunctions, $\tilde{\phi}$ and \tilde{A}_{\parallel} , in an intermediate slab region extending approximately thirty ion gyroradii on either side of the rational surface at $x = 0$. At the edges of this slab region, $\tilde{\phi}$ and \tilde{A}_{\parallel} are required to match onto the ideal MHD solutions which obey the marginal stability equation, Eq. (19), along with $\tilde{E}_{\parallel} = 0$. Specifically, the ratios $(\tilde{A}'_{\parallel}/\tilde{A}_{\parallel})_{MHD}$ are calculated at each edge of the slab region and their values are chosen such that, to leading order

$$\Delta'(a) \equiv \frac{\tilde{A}'_{\parallel}(a)}{\tilde{A}_{\parallel}(0)} \Big|_{MHD} - \frac{\tilde{A}'_{\parallel}(-a)}{\tilde{A}_{\parallel}(0)} \Big|_{MHD} = \Delta_0 \left(1 - \frac{a}{W} \right). \quad (48)$$

Here, $\pm a$ indicates the edges of the intermediate slab region. Hence, the boundary conditions are specified by inputting values of Δ_0 and W . Figure 1 shows a typical plot \tilde{A}_{\parallel} and $\tilde{\phi}$ calculated using the above procedure.

The results from TEDIT and the shooting code agree qualitatively, as previously observed for the case of the finite beta drift wave. Figure 2 depicts the growth rate as a function of the diffusion coefficient as obtained from the two codes. Since both codes are observed to give the same qualitative results, the shooting code is used to generate the numerical data discussed below due to its faster computational speed compared to that of TEDIT.

A plot of $\Delta_0 \equiv \Delta'(x = 0)$ as a function of x_c at marginal stability ($\gamma = 0$) is shown in

Fig. 3 for various values of W . These results agree qualitatively with the analytical formula obtained from the variational calculation which specifies marginal stability to occur when Eq. (48) is satisfied with an equality sign. Solving the above equation for Δ_0 gives

$$\Delta_0 = 2\beta_i \left(\frac{L_s}{L_n} \frac{\tau}{\sqrt{2}} \right)^{1/2} \left(1 - \frac{x_c}{\sqrt{2}W} \right)^{-1}. \quad (49)$$

The plot in Fig. 3 of Δ_0 versus x_c shows the qualitative behavior indicated in Eq. (49). In particular, note that the slope of the curve increases as the parameter W is decreased. Also notice that the value of Δ_0 at which $x_c = 0$ is independent of W .

Figure 4 plots a similar graph of Δ_0 as a function of x_c at marginal stability for several values of β_i . Figure 5 shows the same curve of Δ_0 versus x_c for different values of L_s/L_n . Both figures are in qualitative agreement with expression (49); that is, an increase in either β_i or L_s/L_n leads to a simple vertical displacement of the Δ_0 versus x_c curve.

The variational calculation performed in Sec. IV gave the result of Eq. (45). As is often the case in a variational calculation, one expects the functional dependence of the result with respect to the various parameters involved to be similar to that of the exact solution. The numerical coefficients appearing in the variational solution, however, are only approximations to those of the exact solution whose values can be made more exact by using trial functions closer to the exact eigenfunction. In order to reflect this uncertainty in the numerical coefficients of the variational solution, Eq. (45), two adjustment parameters, α_1 and α_2 , are introduced into the above expression for the growth rate as follows

$$\gamma = \frac{k'_{\parallel} \rho_i v_i^2}{\pi v_e} \left\{ \frac{1}{\beta_i} \Delta'(\alpha_1 x_c) - \alpha_2 \left(\frac{\tau}{\sqrt{2}} \frac{L_s}{L_n} \right)^{1/2} \right\}. \quad (50)$$

where $\Delta'(x) = \Delta_0(1 - x/W)$. Here, α_1 reflects the uncertainty in the variational determination of the magnitude of the value of the parameter a (the edge of slab region about the rational surface) as performed in the calculation of the magnetic terms, \mathcal{L}_A , appearing in Sec. III. Likewise, α_2 reflects the uncertainty in the overall magnitude of the contribution of the electrostatic terms, \mathcal{L}_ϕ , to the variational integral due to such approximations as extending the limits of integration to infinity (see Sec. III). By comparing expression (50) to the numerical data displayed in Figs. 3-5, one can fit this numerical data to a high

degree of accuracy by choosing the values of α_1 and α_2 to be

$$\alpha_1 \simeq 4.5 \quad \alpha_2 \simeq 4/3 \tag{51}$$

Results indicate that α_1 is a weakly dependent function of the ratio x_c/W (α_1 decreases as x_c/W increases). This reflects the fact that the function $\Delta'(x)$ is not strictly a decreasing linear function of x , as approximated analytically ($\Delta'(x) = \Delta_0(1 - x_c/W)$); rather, $\Delta'(x)$ is a function whose slope increases (becomes less negative) as x increases.

In summary, the numerical results obtained from the shooting code agree remarkably well with the analytical expression for the growth rate, Eq. (50), where the parameters α_1 and α_2 are given by Eq. (51). Numerically, the real frequency of the tearing mode is found to be ω_{*e} , which agrees with the analytical predictions.

V. Conclusion

Both numerical and analytical results indicate the tearing mode to have a real frequency equal to the electron diamagnetic frequency and a growth rate given by Eq. (50). The fact that $\omega_r = \omega_{*e}$ indicates that the tearing mode is, in fact, an electron drift wave driven unstable by the equilibrium current gradient. Here, the first term on the right of Eq. (50) is the contribution from the electron magnetic terms and is similar to the basic collisionless tearing mode result¹⁶ ($\gamma \sim \Delta'(0)$) modified to include diffusive electron effects. The second term on the right is the contribution from ion electrostatic terms. Physically, the first term represents the free magnetic energy in the outer region ($|x| > x_c$) available to drive the tearing mode. The second term represents the energy required to maintain the ion motion. Since this mode now has a finite real frequency, energy is needed to sustain the ion motion, whereas in resistive MHD, the mode is purely growing. At low densities the first term dominates, indicating that the tearing mode can be stabilized for sufficiently large values of the electron diffusion coefficient. At high densities, the second term becomes important and consequently the tearing mode can be stabilized for sufficiently high β_i .

Numerical calculations of $\Delta'(x)$ for Alcator-C profiles indicate that $\Delta'(x)$ is a monotonically decreasing function of x with $\Delta'(0) > 0$. Hence, for low densities, stability is obtained for $\alpha_1 x_c > W$, where $\Delta'(W) = 0$ and α_1 is a numerical constant. This stability criterion can be written as $D_e > 3k'_{\parallel} v_e (W/\alpha_1)^3$ with $k'_{\parallel} = mq'/Rq^2$, where the functional dependence of W on the profile quantities must be determined numerically. This equation indicates that increased turbulent electron diffusion stabilizes the tearing mode. Consequently, if $D_e \sim 1/n$, then there exists some critical density below which the tearing mode is stabilized. Theoretically predicted values of the critical density are in approximate agreement with experimental values; however, the experimental scaling⁷ of $n_c \sim B^2$ has not been explicitly derived unless $D_e \sim B^2$. (Note that for the parameters $a = 16\text{cm}$, $L_s/L_n = 16$, $W = 1\text{cm}$ and $T_e = 1\text{Kev}$, then stabilization occurs for $D_e \geq 10^4\text{cm}^2/\text{secs}$).

A related analysis reported by Meiss et al.¹⁷ also treated the problem of the effect of electron diffusion on the tearing mode. They arrived at a very different conclusion, however; namely, that diffusion has virtually no effect on the tearing mode nor did they find

the additional stabilizing term due to ion inertial effects. The results of the present work for the “magnetic” tearing mode (neglecting the effects of a finite electrostatic potential) differ only by the inclusion of the additional physical effect of turbulent smearing of the perturbed current which thus reduces the available energy to the value $\Delta'(\alpha_1 x_c)$. The analysis by Meiss et al., by asymptotically matching an inner solution to an ideal MHD solution at large x , intrinsically contained the full MHD energy, $\Delta'(0)$, and could not consider this effect. Besides the fact that Meiss et al. ignored this the stabilizing phenomena due to the ion inertia, their results agree with the above results of the “magnetic” tearing mode except for the phenomena of turbulent smearing of the perturbed current.

The growth rate as expressed by Eq. (50) also indicates that at high densities, the tearing mode can also be stabilized due to the effects of ion inertia. Assuming the effect of electron diffusion can be ignored, this stabilization takes the form of specifying a critical ion β , above which the tearing mode is stabilized. Setting $x_c = 0$, this critical β is given by

$$\beta_i > \beta_{i_c} \equiv \frac{3}{4} \Delta_0 \left(\frac{\sqrt{2} L_n}{\tau L_s} \right)^{1/2}, \quad \Delta_0 \equiv \Delta'(0). \quad (52)$$

Here, Δ_0 is normalized in units of the ion gyroradius. For typical Iator-C parameters, the above formula indicates that the tearing mode is stable, contrary to experimental observation. (Note that for the parameters $\Delta_0 = 0.1cm$, $\rho_i = 0.03cm$, $L_s/L_n = 16$ and $\tau = 1$, then $\beta_c \simeq 10^{-3}$).

The result of stabilization at ion betas above some critical value, $\beta_c \sim \Delta_0(L_n/L_s)^{1/2}$, was calculated previously by Basu and Coppi⁹ through a kinetic treatment utilizing asymptotic analysis. The work of Basu and Coppi⁹ and of Coppi et al.¹⁸ also modified this result to include the effects of finite temperature gradients in which they found stabilization to occur when the ion beta exceeded a critical value of $\beta_c \simeq .1\Delta_0(L_n/L_s)^2 I_e$. Here I_e is a function of the electron temperature gradient whose magnitude is on the order of unity. This critical ion beta is much lower than that occurring in the absence of temperature gradients, indicating that the effects of finite temperature gradients on the $m = 2$ mode are strongly stabilizing. A recent analysis by Drake et al.¹⁹ based on the Braginski fluid equations including the effects of finite temperature gradients also gave a result of the

form $\beta_c \simeq .1\Delta_0(L_n/L_s)^2 I_e$ for the onset of stabilization. It is interesting to note that the growth given by Eq. (50), neglecting the effects of turbulent diffusion, indicates the $m = 2$ mode to be stable for typical Alcator C parameters. This is especially true if one considers the results cited above which include the effects of finite temperature gradients. In light of this observation, as well as the fact that the above stabilization mechanism is a purely linear effect which has been established in both kinetic and fluid models, indicates that the $m = 2$ modes present in current tokamak experiments are driven unstable by additional effects in conjunction with that of an equilibrium current gradient.

In summary, the tearing mode is stabilized at low densities for sufficiently large values of the turbulent electron diffusion coefficient, D_e , and at high densities stabilization is obtained for sufficiently large values of β_i . For low β_i , in which one can approximate $\gamma \sim \Delta'(\alpha_1 x_c)$, then stability is obtained when $x_c > W$, where $\Delta'(W) = 0$. Provided $D_e \sim 1/n$, this implies that a density threshold must be surpassed before the $m = 2$ tearing mode is observed. Physically, turbulent electron diffusion prevents a perturbed current from forming within a correlation distance, x_c , of the rational surface. Hence, turbulent diffusion cuts into the available magnetic driving energy, Δ' . At high plasma β , the effects of ion inertia become important. At high densities in which the effects of electron diffusion become negligible, then this ion inertia effect implies that the tearing mode is again stabilized for β_i above some critical value. These results indicate that it may be possible for a tokamak experiment to operate in a parameter regime such that the tearing mode is stabilized at all densities due to the combined effects of turbulent diffusive stabilization and ion inertial stabilization. Making this work in practice would be an important step toward the elimination of major disruptions in tokamaks.

References

- 1.) Coppi, B., G. Laval and R. Pellat, *Phys. Rev. Lett.* **16**, 1207 (1966).
- 2.) Schindler, K., in *Magnetic Reconnection in Space and Laboratory Plasmas*, E. W. Hones, Ed., American Geophysical Union, Washington, D. C., 1984.
- 3.) Furth, H.P., J. Killeen and M.N. Rosenbluth, *Phys. Fluids* **6**, 459 (1963).
- 4.) Carreras, B., B.V. Waddell and H.R. Hicks, *Nucl. Fusion* **19**, 1423 (1979).
- 5.) Robinson D.C., and McGuire, *Nucl. Fusion* **19**, 115 (1979).
- 6.) Diamond, P.H., R.D. Hazeltine, Z.G. An, B. A. Carreras and H.R. Hicks, *Phys. Fluids* **27**, 1449 (1984).
- 7.) Granetz, R.S., *Phys. Rev. Lett.* **49**, 658 (1982).
- 8.) Esarey, E., J.P. Freidberg, K. Molvig, C.O. Beasley, Jr. and W.I. Van Rij, *Phys. Rev. Lett.* **50**, 583 (1983).
- 9.) Basu, B. and B. Coppi, *Phys. Fluids* **24**, 465 (1981).
- 10.) Freidberg, J.P., K. Molvig, C.O. Beasley, Jr. and W. Van Rij, in *Plasma Physics and Controlled Nuclear Fusion Research 1982* (IAEA, Vienna, 1983), Vol. I, p. 249.
- 11.) Molvig, K., S.P. Hirshman and J.C. Whitson, *Phys. Rev. Lett.* **43**, 582 (1979).
- 12.) Molvig, K., J.P. Freidberg, R. Potok, S.P. Hirshman, J.C. Whitson and T. Tajima, in *Long Time Predictions in Dynamics*, ed. by W. Horton (Wiley, N.Y., 1982).
- 13.) Beasley, Jr. C.O., K. Molvig and W.I. Van Rij, *Phys. Fluids* **26**, 678 (1983).
- 14.) Adler, E.A., R.M. Kulsrud and R.B. White, *Phys. Fluids* **23**, 1375 (1980).
- 15.) White, R.B., D.A. Monticello and M.N. Rosenbluth, *Phys. Fluids* **20**, 800 (1977).
- 16.) Laval, G., R. Pellat and M. Vuillemin, in *Plasma Physics and Controlled Nuclear Fusion Research*, Proceedings of the 2nd International Conference, Culham, England 1965 (IAEA, Vienna, Austria, 1966), Vol. 2, p. 259.
- 17.) Meiss, J.D., R.D. Hazeltine, P.H. Diamond and S.M. Mahajan, *Phys. Fluids* **25**, 815 (1982).
- 18.) Coppi, B., J. W.-K. Mark, and L. Sugiyama, *Phys. Rev. Lett.* **92**, 1058 (1979).
- 19.) Drake, J.F., T.M. Antonson, Jr., A.B. Hassam, and N.T. Glodd, *Phys. Fluids* **26**, 2509 (1983).

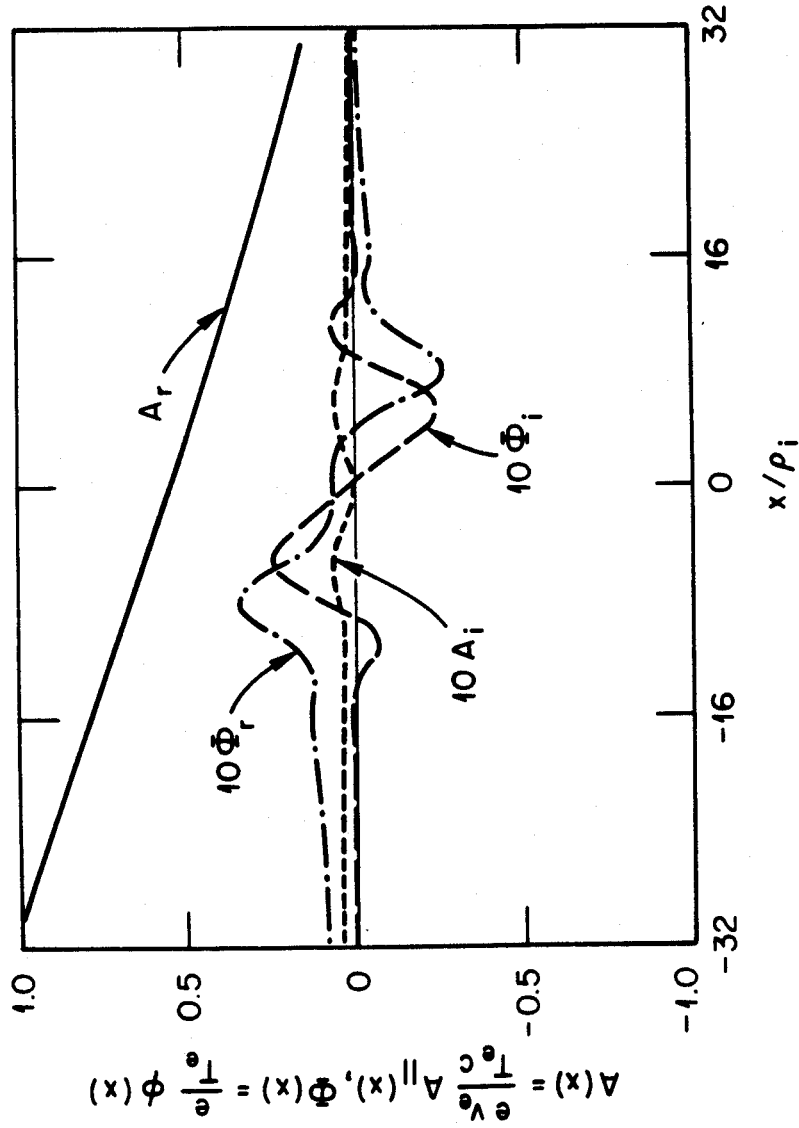


Figure 1. Plots of the perturbed wave potentials, $\tilde{\phi}$ and $\tilde{A}_{||}$, as a function of x . The subscripts r and i refer to the real and imaginary parts, respectively.

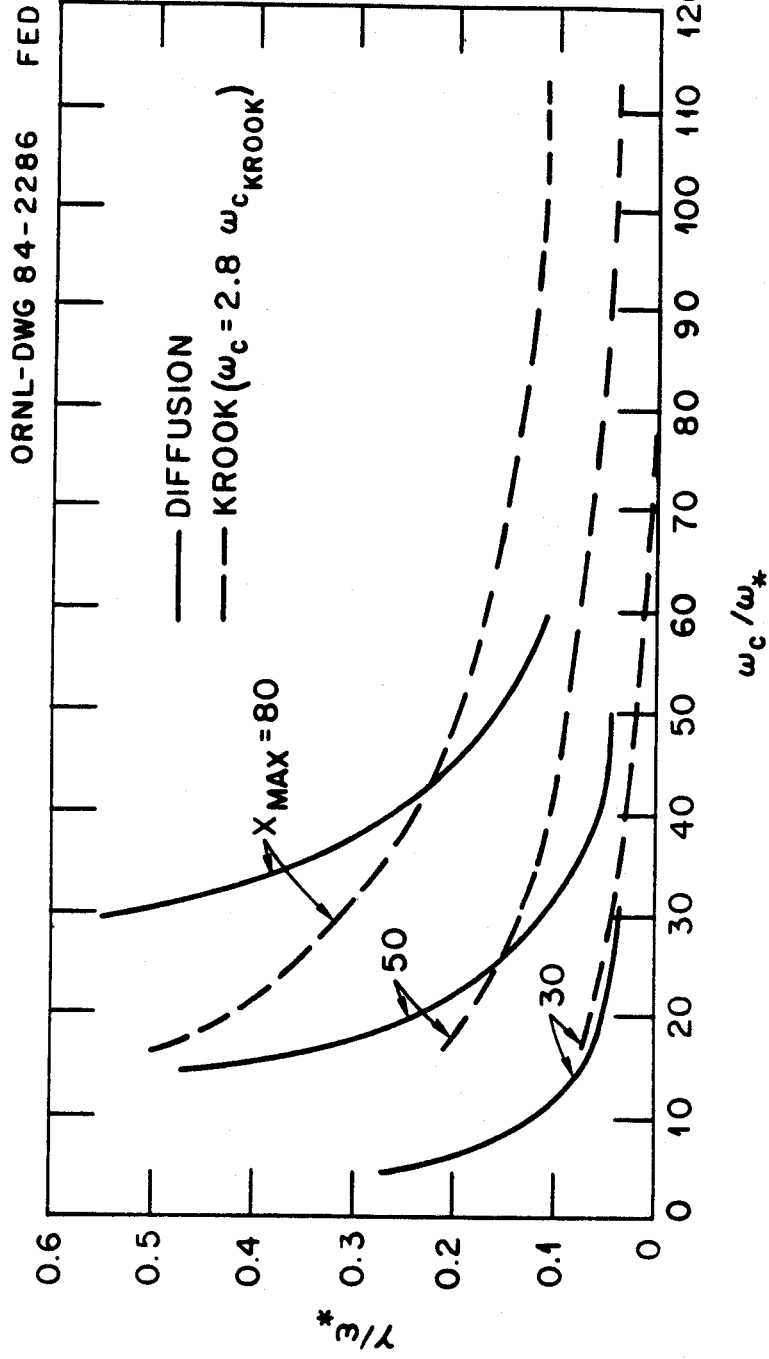


Figure 2. Numerical results for the growth rate comparing the initial value code, TEDIT, using the full diffusion operator, to the shooting code, which uses the Krook approximation. Here the growth rate is plotted for increasing values of the diffusion coefficient (increasing ω_c). The parameter X_{MAX} represents the plasma edge and is a measure of the energy drive, $\Delta'(0)$.

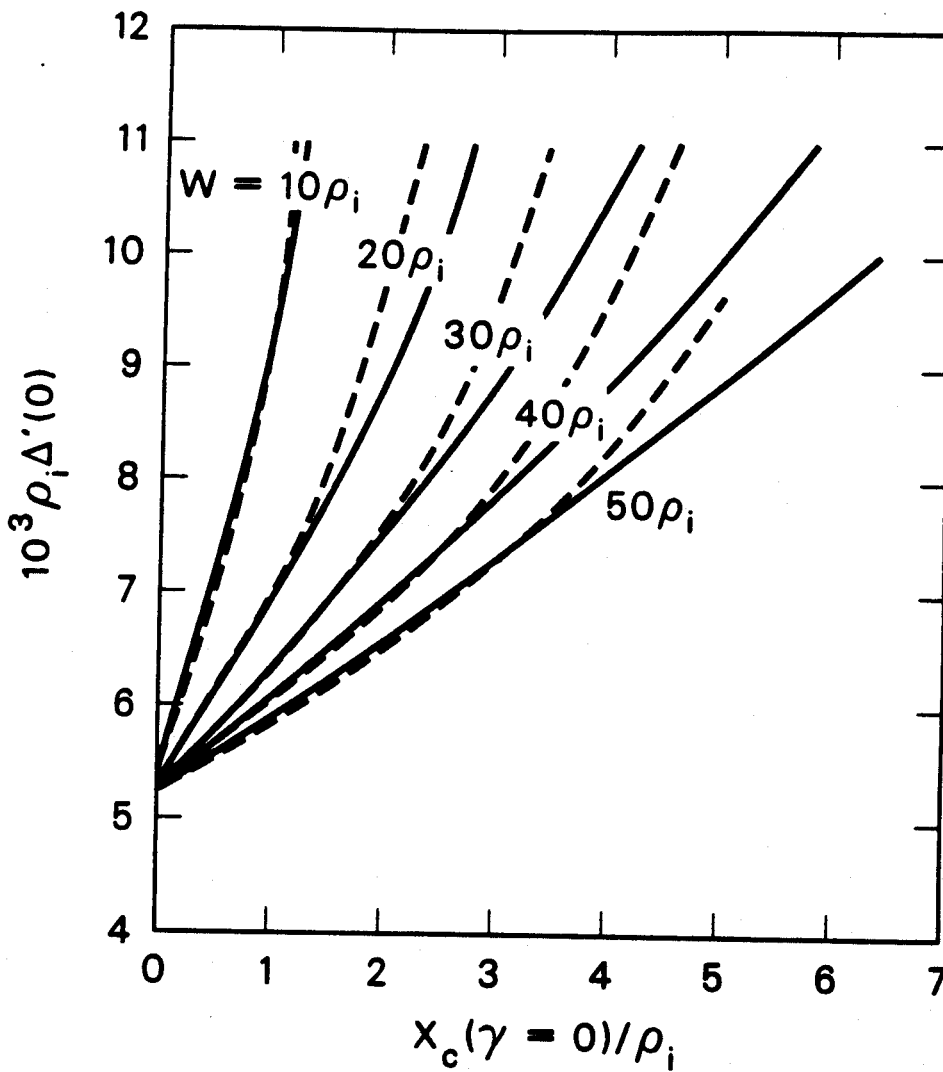


Figure 3.

Plots showing the amount of diffusion (x_c) necessary to obtain marginal stability ($\gamma = 0$) versus given values of free energy ($\Delta'(0)$) for several values of W , where $\Delta'(W) = 0$. The dashed curves are plots of the analytical results indicated by Eq. (49).

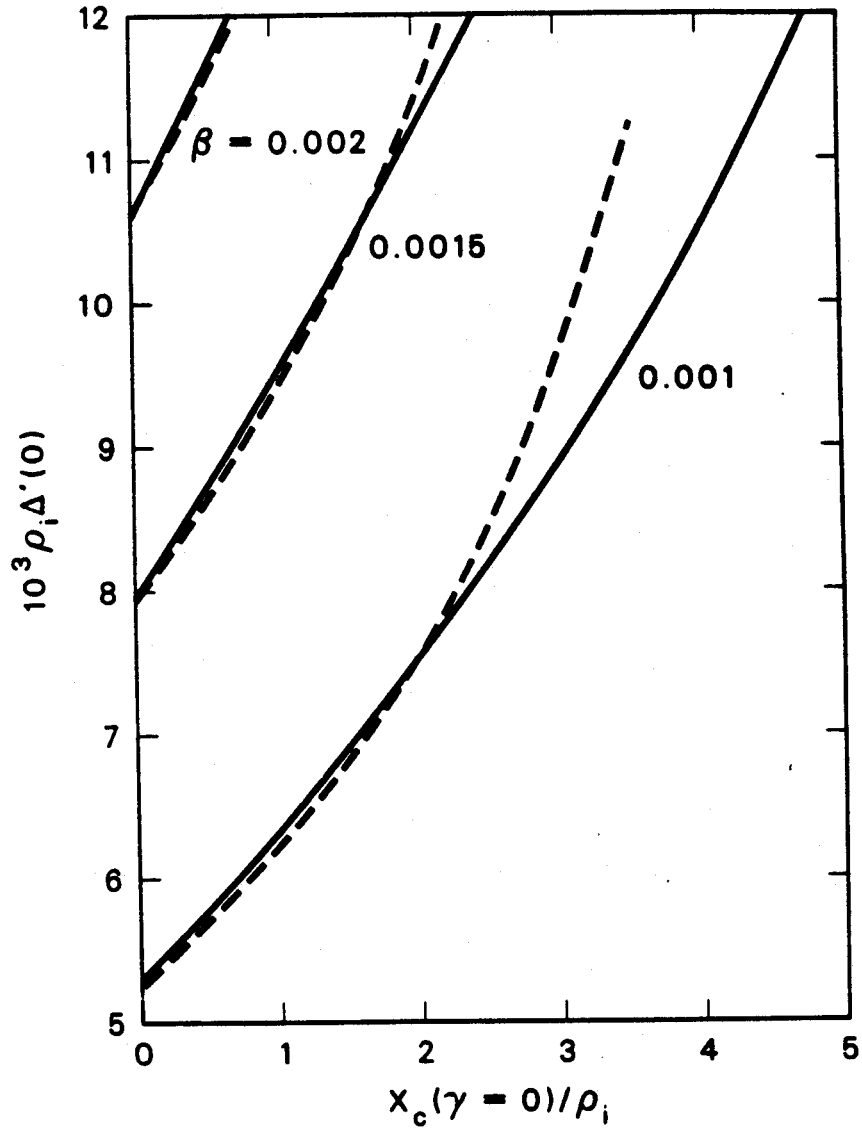


Figure 4.

Plots showing the amount of diffusion (x_c) necessary to obtain marginal stability ($\gamma = 0$) versus given values of free energy ($\Delta'(0)$) for several values of the plasma ion beta, β_i . The dashed curves are plots of the analytical results indicated by Eq. (49).

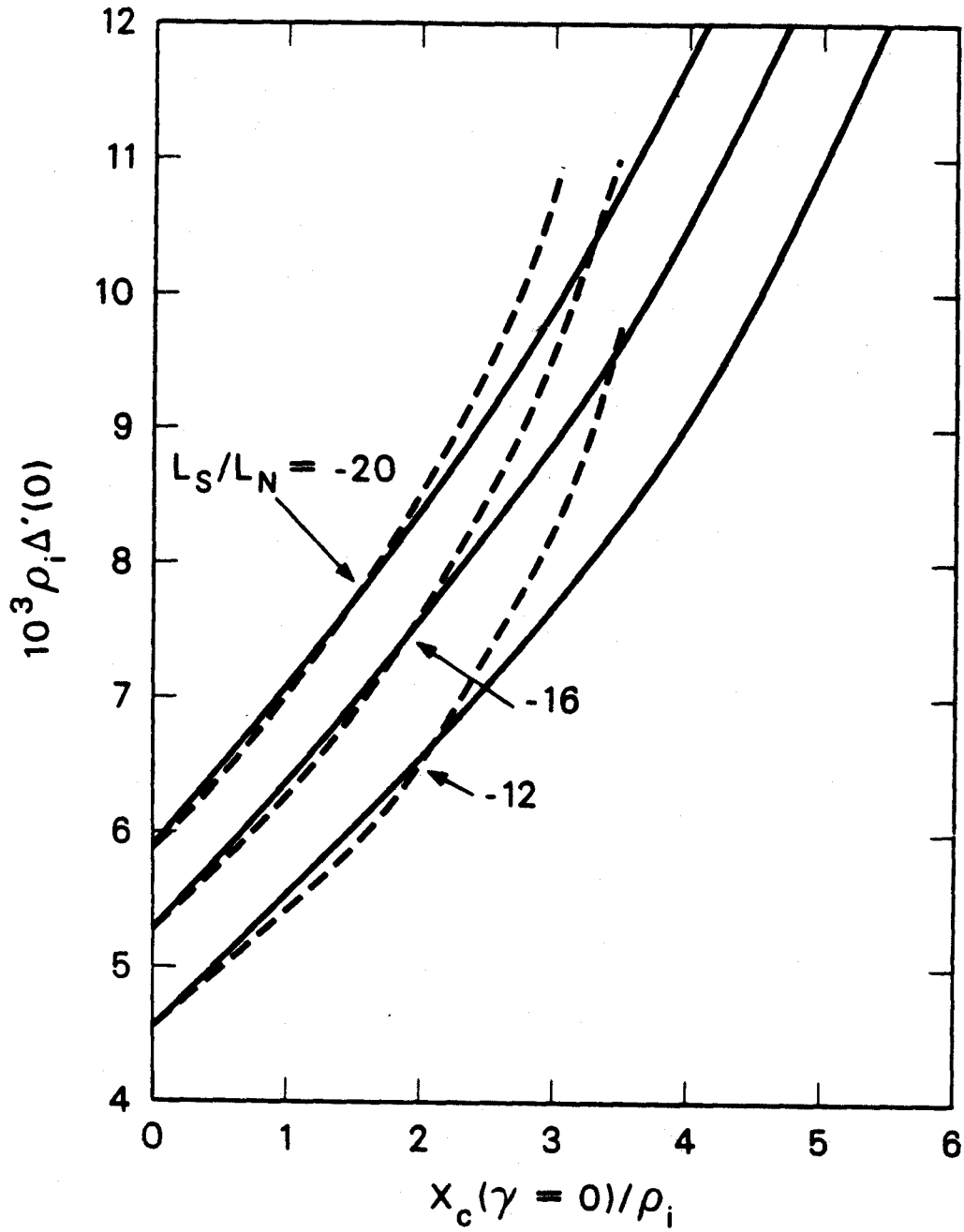


Figure 5.

Plots showing the amount of diffusion (x_c) necessary to obtain marginal stability ($\gamma = 0$) versus given values of free energy ($\Delta'(0)$) for several values of magnetic shear, L_s/L_n . The dashed curves are plots of the analytical results indicated by Eq. (49).